Original Research

Metastatic bladder cancer cells distinctively sense and respond to physical cues of collagen fibril-mimetic nanotopography

James N Iuliano[1,4], Paul D Kutscha[1,4], NJ Biderman[2,4], Sita Subbaram[3], Timothy R Groves[2], Scott A Tenenbaum[1] and Nadine Hempel[1]

[1]Nanobioscience Constellation, College of Nanoscale Science, SUNY Polytechnic Institute, State University of New York, Albany, NY 12203, USA; [2]Nanoengineering Constellation, College of Nanoscale Engineering, SUNY Polytechnic Institute, State University of New York, Albany, NY 12203, USA; [3]Center for Cell Biology and Cancer Research, Albany Medical College, Albany, NY 12209, USA; [4]University at Albany, State University of New York, Albany, NY 12203, USA
Corresponding author: Nadine Hempel. Email: nhempel@sunycnse.com

Abstract

Tumor metastasis is characterized by enhanced invasiveness and migration of tumor cells through the extracellular matrix (ECM), resulting in extravasation into the blood and lymph and colonization at secondary sites. The ECM provides a physical scaffold consisting of components such as collagen fibrils, which have distinct dimensions at the nanoscale. In addition to the interaction of peptide moieties with tumor cell integrin clusters, the ECM provides a physical guide for tumor cell migration. Using nanolithography we set out to mimic the physical dimensions of collagen fibrils using lined nanotopographical silicon surfaces and to explore whether metastatic tumor cells are uniquely able to respond to these physical dimensions. Etched silicon surfaces containing nanoscale lined patterns with varying trench and ridge sizes (65–500 nm) were evaluated for their ability to distinguish between a non-metastatic (253J) and a highly metastatic (253J-BV) derivative bladder cancer cell line. Enhanced alignment was distinctively observed for the metastatic cell lines on feature sizes that mimic the dimensions of collagen fibrils (65–100 nm lines, 1:1–1:1.5 pitch). Further, these sub-100 nm lines acted as guides for migration of metastatic cancer cells. Interestingly, even at this subcellular scale, metastatic cell migration was abrogated when cells were forced to move perpendicular to these lines. Compared to flat surfaces, 65 nm lines enhanced the formation of actin stress fibers and filopodia of metastatic cells. This was accompanied by increased formation of focal contacts, visualized by immunofluorescent staining of phospho-focal adhesion kinase along the protruding lamellipodia. Simple lined nanotopography appears to be an informative platform for studying the physical cues of the ECM in a pseudo-3D format and likely mimics physical aspects of collagen fibrils. Metastatic cancer cells appear distinctively well adapted to sense these features using filopodia protrusions to enhance their alignment and migration.

Keywords: Nanotopography, metastasis, bladder cancer, collagen fibril, nanotechnology

***Experimental Biology and Medicine* 2015; 240: 601–610. DOI: 10.1177/1535370214560973**

Introduction

Metastatic spread remains one of the major reasons for the high death rate due to cancer. Accordingly, survival statistics for metastatic disease remain low. A prominent example of this is bladder cancer, where patients diagnosed with localized tumors have a 95% five-year survival rate. This drops to 36% if the cancer has metastasized regionally, and a devastatingly low 6% after the tumor has spread to distant organs, such as lymph, liver, or bone.[1] Metastatic lesions are difficult to detect, isolate, and treat successfully, and there is a need for better understanding of the multiple steps involved in metastatic progression. These include a cell's ability to migrate, invade, and survive in the extracellular matrix (ECM). Increasingly, it is becoming apparent that physical cues have a prominent role in determining a cell's ability to circumnavigate its environment and that this interaction regulates migration, invasion, and survival. Cells migrating in 3D ECMs display distinct morphology, migratory behavior, and cellular signaling than cells migrating on traditionally studied 2D flat surfaces. For example, compared to movement over flat surfaces, cells migrating in a 3D matrix do not display broad lamellipodia, but rather exhibit smaller width protrusions with increased number and size of pseudopodial extensions.[2–5] Further, it appears that metastatic tumor cells have adapted to reshape and utilize the ECM as "guides" for directed movement. For example, the ECM surrounding locally invasive mammary tumor lesions is reordered by

cancer cells into a radial pattern allowing cells to utilize collagen fibrils as guides to move perpendicularly out from the primary tumor.[6] While researchers have historically relied heavily on studying cancer cell migration on essentially flat (i.e. 2D) surfaces, it is clear that cellular morphology and signaling events are drastically different in 3D environments and there is a need to explore novel surfaces that can mimic these environments.

Three-dimensional physical features of the ECM are frequently of the "nano" scale (typically <100 nm) . Collagen is the most abundant ECM protein and forms fibrils with diameter ranges between 10 and 500 nm, depending on the tissue and the amount of crosslinking and alignment.[2,4] Collagen fibrils within the ECM of tumors have been reported to have diameter ranges between 50 and 200 nm, with a median size close to 60 nm.[7,8] For a structured surface to act as a useful mimic of the ECM, it should initiate the same cellular signaling responses as the 3D environment. In the present study, we set out to examine if mimicking the structural dimensions of collagen fibrils will influence cellular behavior by utilizing nanoscale silicon etched lined surfaces as "pseudo-3D surfaces." This study demonstrates that metastatic tumor cells distinctively respond to sub-100 nm lines and use these as instructive surfaces for alignment and migration.

Materials and methods

Nanoscale lined topography

Etched silicon wafers containing lined nanotopography were obtained from the SUNY Polytechnic Institute College of Nanoscale Engineering. Reactive ion etched silicon wafers with varying dimensions of line diameters and pitches were used to assess alignment of cancer cells. Topographical patterns used are displayed in Figure 1. For subsequent experiments and to more closely mimic collagen fibril dimensions, 65 nm wide lines with 65 nm wide trench line features were created on SiO_2 by either immersion lithography (benzocyclobutene resin and photoresist coating) or reactive ion etch. Alignment and migration did not differ significantly between the two surface modifications. Silicon wafers were cut to fit standard sized tissue culture ware and sterilized using 70% ethanol, followed by ultraviolet light exposure for 30 min, prior to seeding cells.

Cell lines and culture

The non-metastatic 253J bladder cancer cell line and a metastatic derivative cell line 253J-BV were generously provided by Dr Badar Mian (Albany Medical College) and Dr Colin Dinney (M.D. Anderson Cancer Center) and cultured in Dulbecco's Modified Eagle Medium (CellGro) with 10% fetal bovine serum (FBS, Hyclone) in a humidified 37°C incubator, 5% CO_2.[9,10] The 253J cell line was obtained from a human bladder cancer patient, and the highly metastatic 253J-BV cell line derived from these following five successive transplantations in the bladders of nude mice.[11]

Scanning electron microscopy (SEM)

Cells grown on silicon wafers containing lined nanotopographies were fixed using a 3% glutaraldehyde (Sigma Aldrich, St. Louis, MO) solution in potassium phosphate buffer, pH 7.4, with 1.0 M sucrose for 2 h at room temperature. The sample was then dehydrated with 50, 70, 80, 95, and 100% ethanol solutions and dried overnight prior to imaging. After fixation, cells were sputter coated with 5 nm gold/palladium (Denton Vacuum Desk IV). Fixed samples were imaged using Nova-600 ESEM (FEI) using high vacuum and LEO 1550 SEM (Zeiss). Cells were imaged using the in-lens detector at high vacuum with 1 keV accelerating voltage. Cell alignment on the nanoscale topographies was quantified by drawing a line from the center of the cell to the edge of each protrusion; this was repeated for each cell on the lined patterns with multiple protrusions being included in the measurement (Figure 1(c)). Cells were considered aligned if at least two lamellipodia protrusions were within 10° of the orientation of the line direction.

Immunofluorescence staining

Cells were fixed in 4% paraformaldehyde, permeabilized using 1% Triton X100, and blocked in 3% FBS in PBS. Actin cytoskeleton was stained using Phalloidin Texas Red (1:50 dilution in PBS). Phosphorylated focal adhesion kinase (FAK) at tyrosine-397 was stained using Phospho-FAK (Y397) Antibody (Cell Signaling), followed by secondary antibody incubation with Alexa-Fluor 488 (Life Technologies). Cells on silicon wafers were mounted on a No. 1.5 glass coverslip using Prolong Gold Antifade (Invitrogen) and sealed. Samples were imaged using Axio Observer (Zeiss) with Colibri LED light source or using AMG Evos FL (Life Technologies). Cells were considered aligned if at least two lamellipodia protrusions were within 10° of the orientation of the line direction. Cell protrusions were measured from the nucleus (stained with DAPI, DAPI staining not shown in Figure 2) to the tip of the protrusion and the angle measured relative to the direction of the topography measured. Overlapping cells or cells with non-discernable cell junctions were disregarded in the measurement.

Migration assays

Migration was assessed by scratch wound healing assays.[9] A wound was introduced into a confluent monolayer using the end of an inoculating loop, and cells were allowed to migrate over the course of 8 h prior to fixation. Cells were visualized using phalloidin staining for actin (as described earlier) and migration was quantified by measuring the area of wound that remained uncovered by cells after 8 h.

Filopodia quantification

Cells grown on 65 nm lined etched silicon were evaluated for filopodia formation, using flat silicon as a control. Cells were seeded at 50% confluence and allowed to attach overnight, after which samples were fixed for SEM as described earlier. Using ImageJ (NIH), the length of cell edge and filopodia was measured using a scale calibrated to the scale bar in the image and filopodial protrusions counted using the cell counter plug-in. Filopodia numbers were represented as the number of filopodia divided by the total cell perimeter.

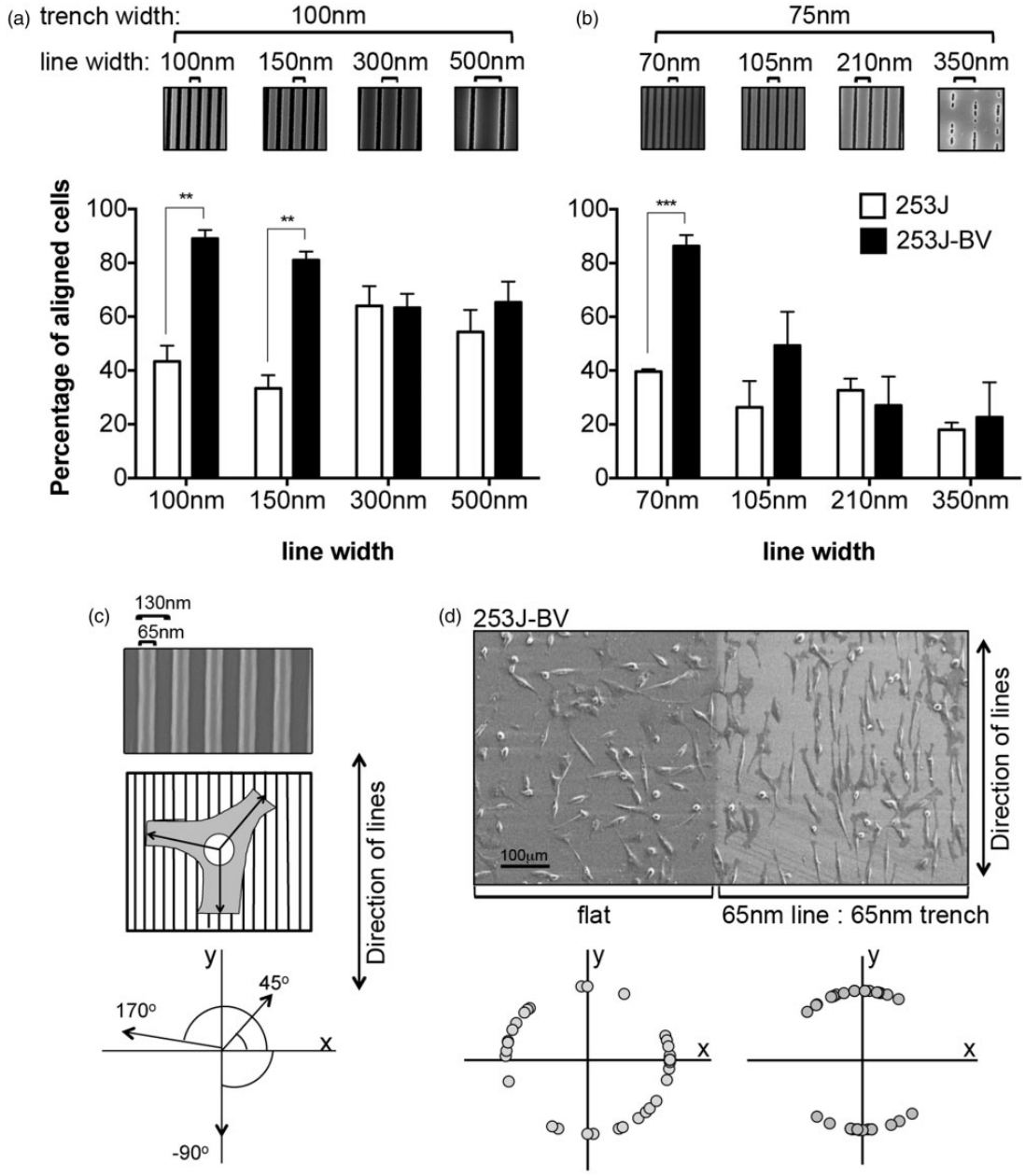

Figure 1 Nanoscale lines below 150 nm can differentiate metastatic 253J-BV from non-metastatic 253J cells based on anisotropic behavior. (a and b) Non-metastatic 253J and metastatic 253J-BV cells were grown to subconfluency on silicon wafers containing varying lined topographical patterns. Cells were analyzed for anisotropic behavior on the increasing nanoscale line widths with fixed trench size of 100 nm (a) or 75 nm (b) trenches. SEM images of the surfaces are shown above the alignment graphs. Graphs represent percentage of alignment of 20–30 cells per pattern from three replicative experiments (mean ± SEM; $^{**}p < 0.01$, $^{***}p < 0.001$, Student's *t*-test). (c) Upper panel shows SEM image of 65 nm lined features (created using photoresist immersion lithography) used in (d). Lower panels show schematic of lamellipodial protrusion directionality measurements. (d) 253J-BV metastatic cells were grown on 65 nm lines, adjacent to a region of unpatterned photoresist (Scale bar = 100 μm). Random orientation of cells is observed on the flat region while alignment to nanoscale topography is observed on the 65 nm lines. Lamellipodia directionality was plotted using polar coordinates of the lamellipodial protrusion angle (n = 20–30 cells, 2–4 protrusions per cell)

Statistical and quantitative analysis

ImageJ (NIH) was used for image analysis in alignment and migration assays. Data were analyzed and plotted using Xcel and Graph Pad Prism software (v6). Student's *t*-tests were performed to assess significance. All data are represented as mean ± standard error of the mean and are representative of at least three replicate experiments.

Results

Metastatic bladder cancer cells display enhanced alignment to lines that mimic physical dimensions of collagen fibrils

To discern whether the dimensions of nanotopographical lined features influence metastatic 253J-BV and non-metastatic 253J bladder cancer cell line behavior, cells were cultured below confluence on two silicon-etched arrays of

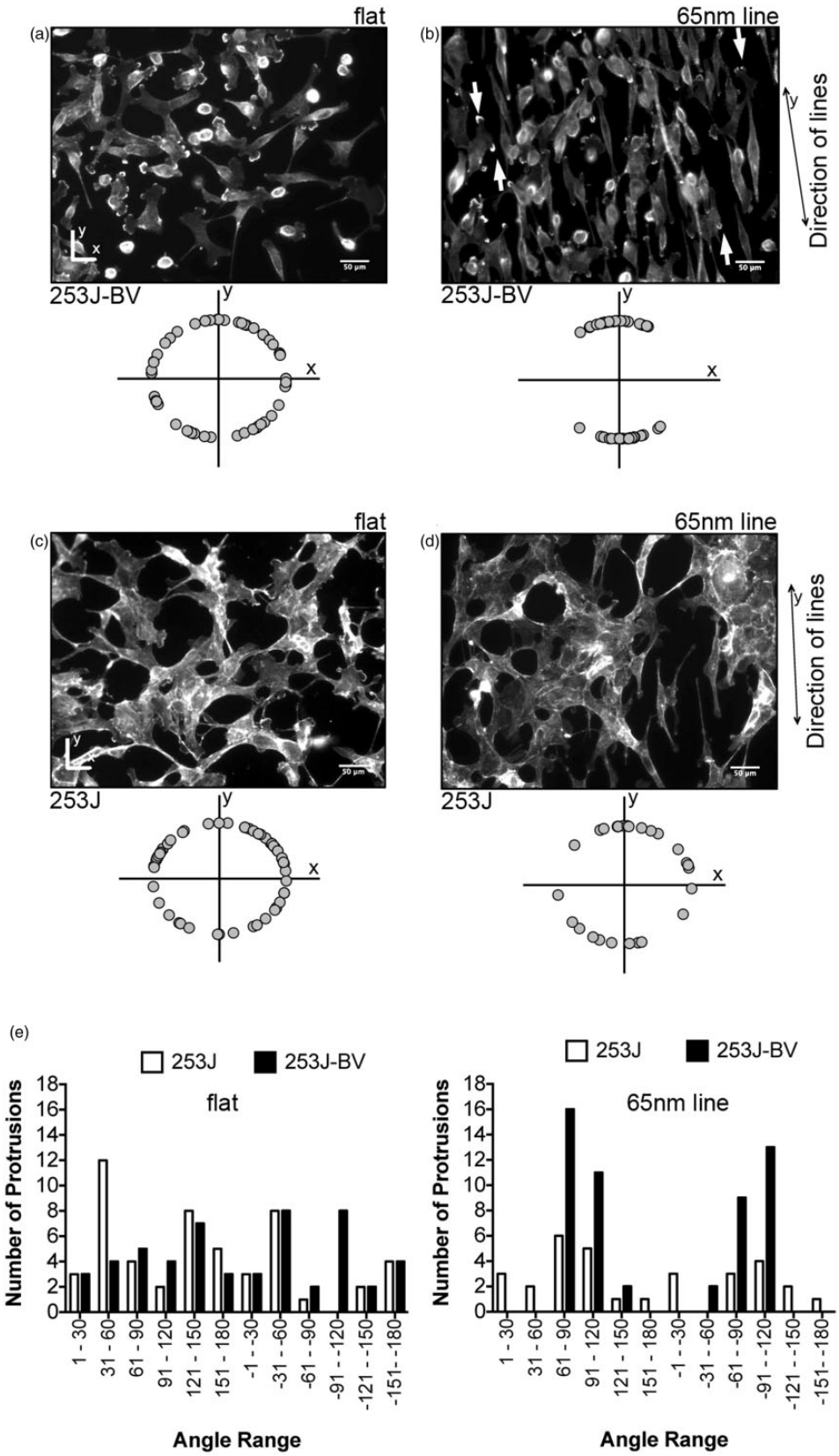

Figure 2 Sixty-five nanometer lines determine the direction of lamellipodial protrusions only in metastatic bladder cancer cells. Metastatic 253J-BV (a and b) and non-metastatic 253J cells (c and d) were grown on flat (a and c) or 65 nm photoresist-patterned surfaces (b and d; scale bar = 50 μm). The actin cytoskeleton was visualized using Phalloidin Texas Red and the directionality of lamellipodial protrusions quantified from 20 to 30 cells. A high degree of lamellipodia alignment was observed in the 253J-BV metastatic cells on the 65 nm lines (b) compared to the random orientation of the metastatic cells grown on flat photoresist surfaces (a). Little alignment of 253J lamellipodia was observed on 65 nm lines (d). White arrows in panel B highlight actin ruffling at the lamellipodial fronts of 253J-BV cells on 65 nm lines. (e and f) Frequency of lamellipodial protrusion angles on flat surfaces and 65 nm lined topography (n = 26–56 lamellipodial protrusion from 20 to 30 cells). Angles were measured as highlighted in Figure 1(c)

lined topography ranging in line widths from 70 to 500 nm (Figure 1(a) and (b)). Each array contained four feature sizes with increasing line width, but constant between-line trench size (100 nm [Figure 1(a)] or 75 nm [Figure 1(b)]). These submicrometer dimensions were chosen to mimic the reported diameters of collagen fibrils. Metastatic 253J-BV bladder cancer cells displayed significant anisotropic behavior on lined topography that closely mimicked the diameter of collagen fibrils, with the strongest alignment observed on feature sizes at $\leq$150 nm with a 1:1 or 1:1.5 trench ratio. These features were also able to best differentiate metastatic from non-metastatic cells based on their unique ability to align to the direction of the lines. Non-metastatic 253J cells showed no appreciable enhancement of anisotropy to these features.

To further study the difference in cellular behavior between metastatic 253J-BV cells and its non-metastatic parental variant 253J on patterns that resemble collagen fibril dimensions, subsequent studies were carried out with an etched silicon wafer patterned with 65 nm wide lines separated by 65 nm trenches (100 nm line height; Figure 1(c)). Strong alignment of the 253J-BV cells was again observed on the 65 nm line patterns compared to adjacent flat, non-etched surfaces (Figure 1(d)). The angle of the lamellipodial protrusions was plotted using polar coordinates (Figure 1(c)) and lamellipodia showed a high degree of directionality with the 65 nm lines (Figure 1(d)). A much wider distribution of protrusion angles was observed on the adjacent flat region.

Staining of the actin cytoskeleton with fluorescently labeled phalloidin, we were able to visualize alignment and lamellipodial protrusion directionality by mounting cells grown on silicon wafers onto glass cover slips. As in Figure 1(c) lamellipodial protrusion directionality was measured and plotted using polar coordinates in an x–y plane. As in Figure 1, fluorescence labeling of actin further demonstrated enhanced alignment of 253J-BV cellular protrusions along the 65 nm lines compared to random distribution on flat surfaces (Figure 2(a) and (b)). In comparison, non-metastatic 253J bladder cancer cells showed little increase in alignment on 65 nm lines relative to flat surfaces (Figure 2(c) and (d)). 253J cells had a higher propensity to cluster with other cells on both surfaces, whereas 253J-BV cells presented more frequently as single cells, a phenotype that was enhanced on the 65 nm lines. In addition, nanotopographical lines induced the formation of lamellipodial ruffles at the polar ends of 253J-BV cells, a common feature of migrating cells (Figure 2(b)).

Nanoscale lined patterns act as guides for migration

Collagen fibrils have been shown to enhance cell movement and act as physical guides for migrating cancer cells.[6] In order to test if lined nanotopography can mimic the physical dimensions of collagen fibrils and similarly induce a migratory phenotype in metastatic bladder cancer cells, a scratch wound healing assay was carried out on 253J and 253J-BV cells cultured as monolayers on the 65 nm lined patterns. Wounds were scratched parallel to the line direction or perpendicularly across the 65 nm lines to compare migration of cells perpendicular (Figure 3(a) and (e)) or parallel (Figure 3(b) and (f)) to the features, respectively. 253J-BV cells were previously shown to have enhanced migration compared to 253J cells on flat surfaces.[9] Interestingly, 253J-BV migration parallel to the lines (Figure 3(b)) was significantly faster than perpendicular to the lines (Figure 3(a)), as indicated by a reduction of the open wound area following 8 h of migration (Figure 3(i)). Although non-metastatic 253J cells also increased their migration along the features this was less dramatic (Figure 3(j)). These data suggest that lined features that mimic the physical dimensions of collagen fibrils act as cues to determine the directionality of cellular movement and that this is a characteristic specific to metastatic tumor cells. Closer inspection of the organization of the cytoskeleton of cells at the leading edge of the wound revealed that the actin cytoskeleton conformed to the direction of the underlying topography, which was more evident for 253J-BV cells than the non-metastatic 253J cells (Figure 3(c), (d), (g) and (h)). These data suggest that feature-guided alignment of the actin cytoskeleton at 90° to the wound may prevent efficient migration of tumor cells across the 65 nm lines.

Nanoscale lines induce formation of filopodia protrusions

Enhanced filopodia turnover is associated with increased migration of metastatic tumor cells.[12] To elucidate the mechanisms behind enhanced alignment and migration of metastatic 253J-BV cells on 65 nm lined features, we examined the formation of filopodial protrusions using SEM (Figure 4). Quantification of the number of filopodia per μm of cell perimeter revealed that 253J-BV cells on 65 nm lines formed significantly more protrusions than cells cultured on flat surfaces (Figure 4(e)). Compared to cells grown on flat silicon surfaces (Figure 4(a) and (b)), 253J-BV cells cultured on 65 nm lined surfaces displayed many filopodia along the axis of the cell body which were directed perpendicular to the underlying 65 nm lines (Figure 4(c) and (d), black arrows). Small filopodia protrusions perpendicular to the cell body were also observed on flat surface albeit the numbers of these were far less than on the lined topography. In contrast, long filopodia were observed at the lamellipodial fronts of the cells (Figure 4, white arrows). Importantly, the length of 253J-BV filopodia at the leading edge was significantly enhanced by the presence of the underlying topographical features, with cells grown on 65 nm lines displaying filopodia on average 2.2-fold longer than cells cultured on flat surfaces (Figure 4(f)). Comparing filopodia numbers between the cell body and the leading edge revealed that lamellipodia contained on average more filopodia than the cell body under both flat and lined topography. The frequency of filopodia per μm cell perimeter increased proportionally at both the leading edge and along the cell body when cells were grown on 65 nm lines (Figure 4(g)); however, the lined topography did not induce significantly higher lamellipodial numbers at the leading edge. These data suggest that 65 nm lined topography increases the frequency of filopodia formation

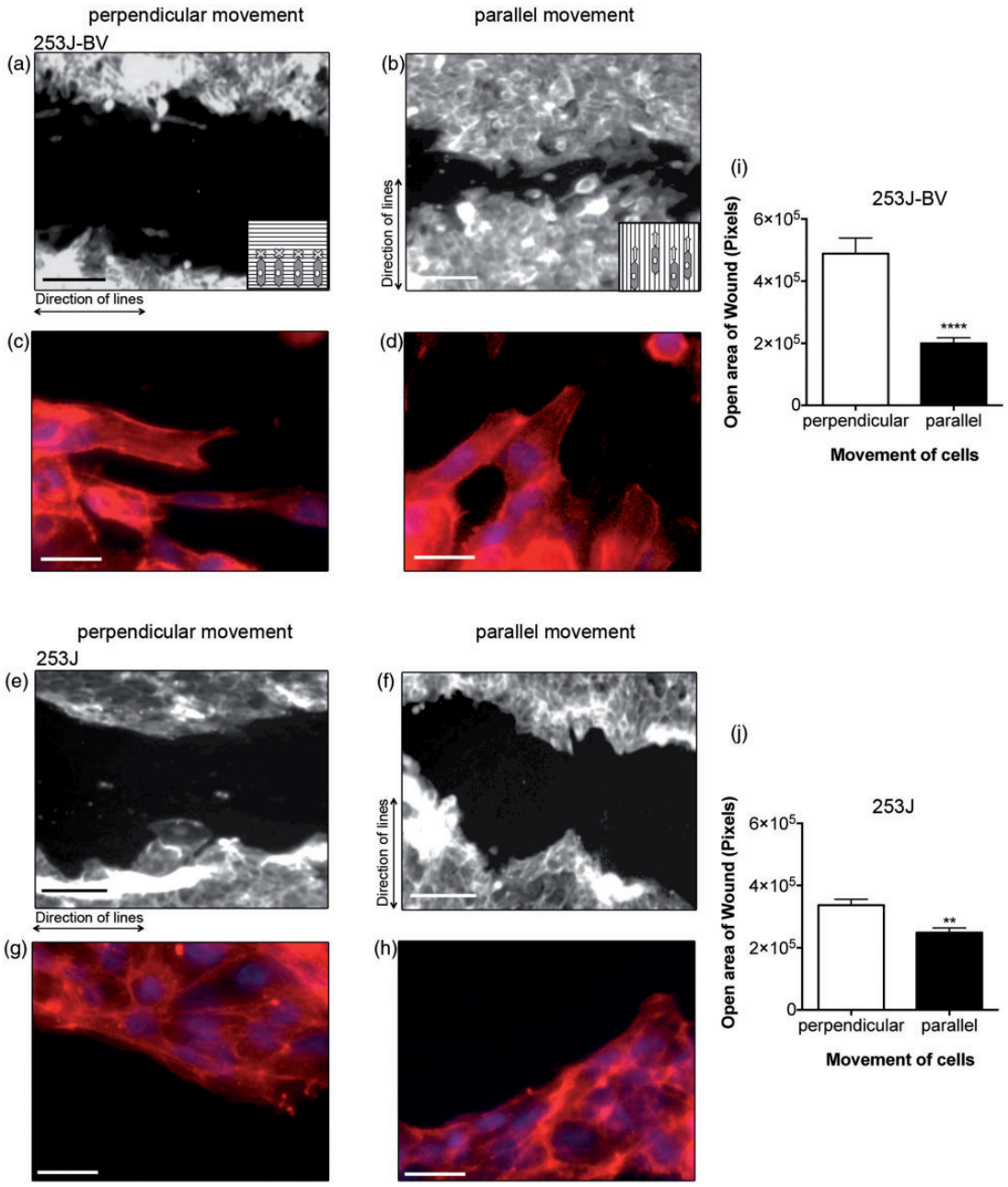

Figure 3 Direction of nanotopography determined directionality of metastatic tumor cell migration along. Metastatic 253J-BV (a to d) and non-metastatic 253J cells (e to h) were grown on 65 nm photoresist-patterned surfaces and allowed to grow to confluence (scale bar = 100 μm). Wounds were introduced into the monolayer to allow cellular movement perpendicular (a, c, e, g) or parallel (b, d, f, h) to the lines. Cells were allowed to migrate for 8 h, followed by fixation, staining for actin cytoskeleton with phalloidin (as in Figure 2). Phalloidin staining indicates that the actin cytoskeleton conforms to the directionality of the wound (253J-BV: c, d; 253J: g, h; Scale bar 20 μm). Wound closure was monitored by measuring the remaining open wound area (i and j; n = 12–16; mean ± SEM; $^{**}p < 0.01$, $^{****}p < 0.0001$, Student's *t*-test)

along the cell body and increases the length of filopodial protrusions at the leading edge.

Nanoscale lines enhance focal contact formation and stress fiber formation in metastatic bladder cancer cells

In addition to the induction of filopodia, metastatic 253J-BV cells also displayed enhanced formation of focal contacts along the lamellipodial front when grown on 65 nm lines, compared to flat surfaces (Figure 5(a) to (h)). This was visualized by immunofluorescence analysis of Phospho-FAK (Y397). The appearance of small punctate phospho-FAK events is an indication of small focal contacts, which are more dynamic than mature focal adhesions and present in migrating cells. Further, 65 nm lines clearly induced actin stress fiber formation along the axis of the 253J-BV cells (Figure 5(e) and (g)). These events are necessary for migration of cancer cells and our data suggest that features mimicking the physical dimensions of collagen fibrils are sufficient to induce a pro-migratory phenotype in

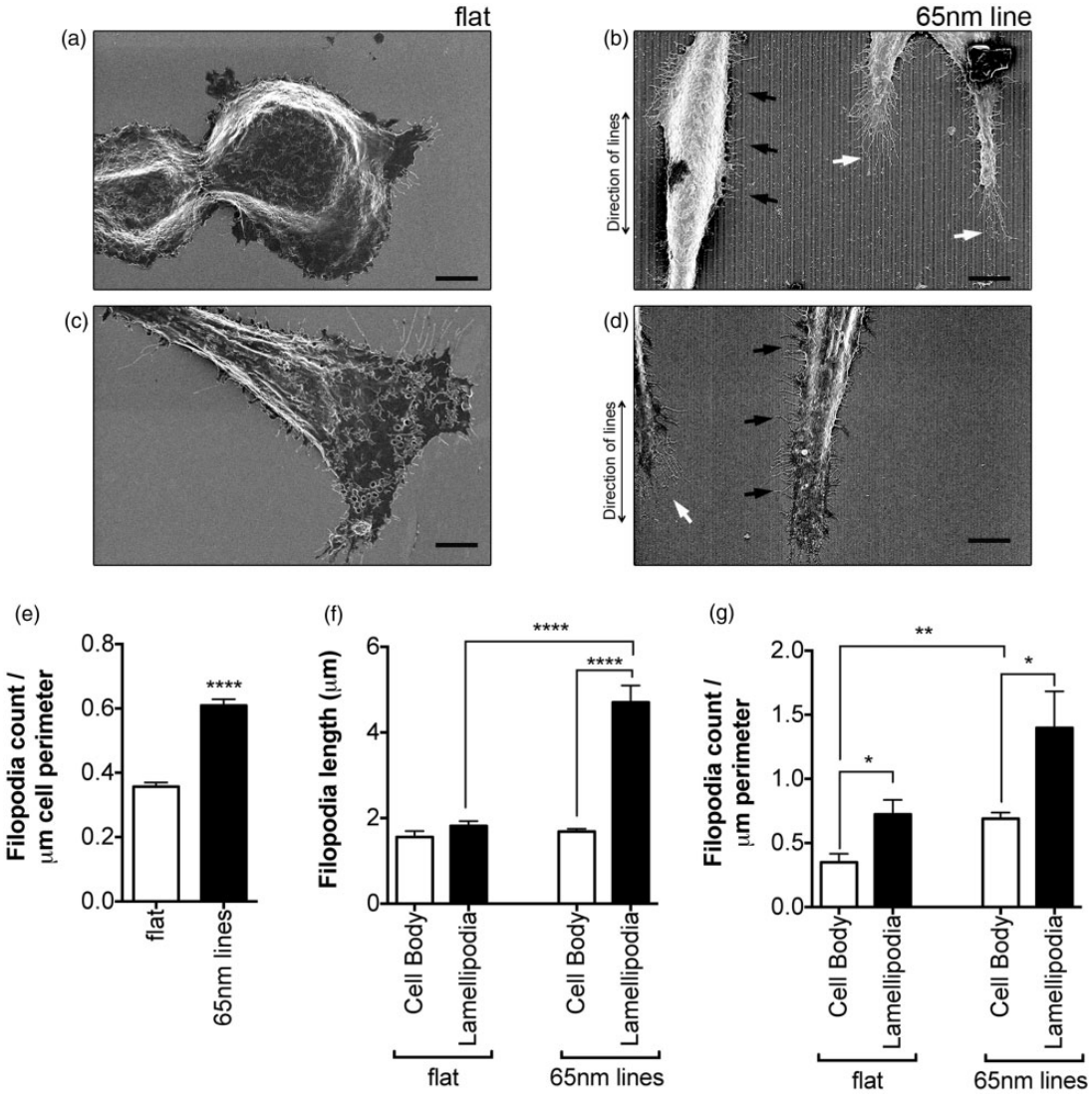

Figure 4 Nanoscale lines induce filopodia formation. SEM images of 253J-BV metastatic bladder cancer cells cultured for 24 h on flat silicon wafer surface (a and b) or 65 nm reactive ion-etched lines (c and d; scale bar = 5 μm). Black arrows highlight many small filopodia perpendicular to the cell body and lined features. White arrows show longer radial filopodial protrusions emanating from the lamellipodial front. The total number of filopodia per length of cell perimeter (μm) was quantified (E; n = 53–59 cells; mean ± SEM; ****$p < 0.0001$, Student's *t*-test). (f) Lengths of filopodia on either the leading lamellipodial edge or the cell body were measured and compared between cells grown on flat or 65 nm topography (n = 6 cells, 89–143 filopodia quantified, mean ± SEM; ****$p < 0.0001$, Student's *t*-test). (g) The number of filopodia per length of lamellipodial front or cell body perimeter (μm) was counted and quantified from six cells (mean ± SEM; *$p < 0.05$, **$p < 0.01$, Student's *t*-test)

metastatic tumor cells. In contrast, non-metastatic 253J cells displayed broad phospho-FAK staining along the perimeter of the whole cell, indicative of mature focal adhesions and cells that are less migratory (Figure 5(i) to (l)). This pattern was not significantly altered when 253J cells were grown on 65 nm lines.

Discussion

Given that many of the functionally relevant aspects of the ECM are comprised of nanometer scale structures and that these can regulate cancer cell behavior, the aim of our study was to utilize nanotopography to mimic the dimensions of collagen fibrils and to assess if this could discriminate metastatic from non-metastatic tumor cells. Using a pseudo-3D topographical surface patterned with 65 nm wide lines our data show that metastatic tumor cells can uniquely sense this pattern and respond by enhancing anisotropy and migration. Metastatic bladder cancer cells (253J-BV) appear to be able to sense and align to nanoscale lined patterns with width dimensions less than 100 nm (Figures 1 to 3), which is on the scale of collagen fibrils in the ECM.[13,14] The non-metastatic bladder cancer parental cells (253J) show reduced alignment to the 100 nm lines compared to the 253J-BV. On lined patterns where the line size was 3–5 times larger than the trench size, both bladder cancer cell types showed random orientations consistent with that of a flat surface. We also observed that there was a lower limit to the alignment of metastatic tumor cells. Both cell lines showed minimal adhesion to 48 nm line patterns (data not

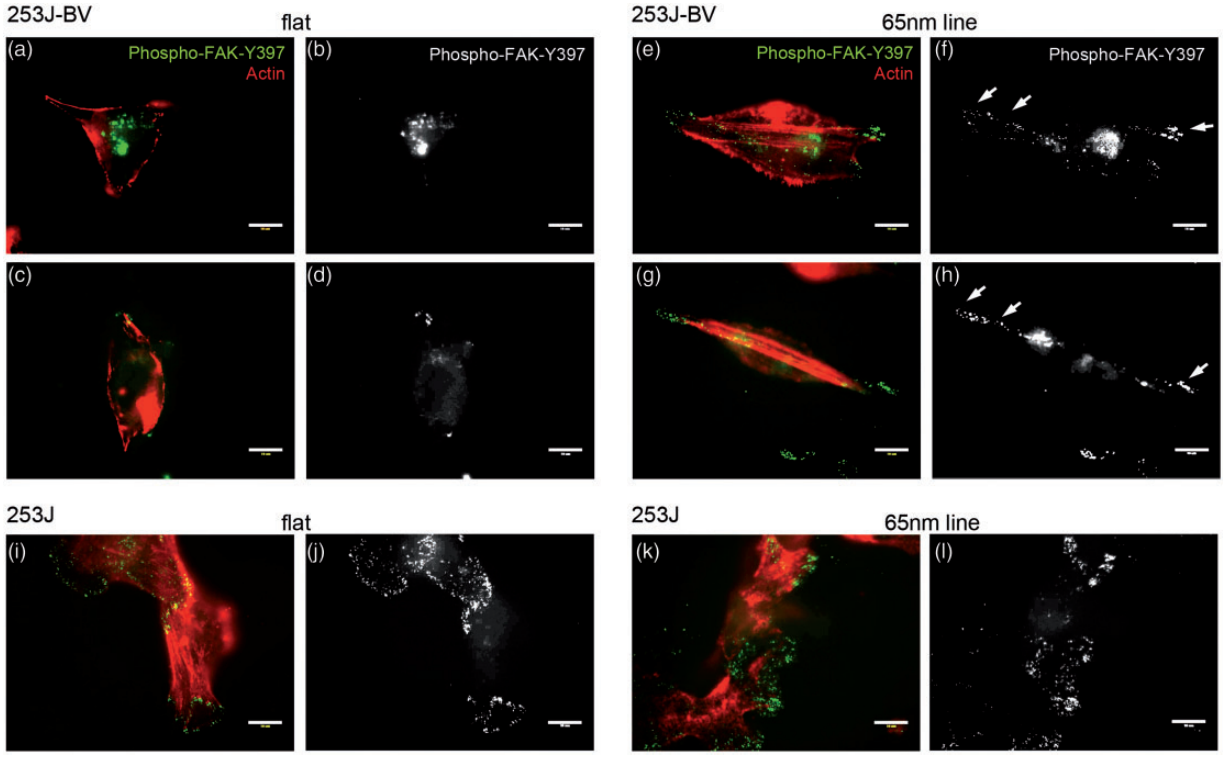

Figure 5 Nanoscale lines promote focal contact and stress fiber formation in metastatic tumor cells. Metastatic 253J-BV (a to h) and non-metastatic 253J cells (i to l) were grown on flat silicon wafer surface (a to d and i, j) or 65 nm reactive ion-etched lines (e to h and k, l; scale bar = 10 μm). Following fixation, cells were immunofluorescently labeled for phospho-FAK (Y397, green) and stained for actin with phalloidin (red). White arrows indicate small focal contacts, as indicated by phospho-FAK-Y397 staining, along the axis and front of 253J-BV lamellipodia on 65 nm lines

shown), and it was therefore concluded that the optimal patterns that discriminate metastatic from non-metastatic bladder cancer cells are those that have similar dimensions to those of collagen fibrils commonly found in the ECM (~65–100 nm) at a 1:1 line width to trench size.

A number of studies have demonstrated anisotropic alignment of other cell types on nano and micro-scale topography, including fibroblasts,[15] corneal epithelial,[16–18] mesenchymal stem,[19] osteoblast,[20,21] myoblasts,[22] and vascular endothelial cells.[23] Many of these cell types were unable to align to lined topography with widths <100 nm, which together with our data suggests that metastatic tumor cells uniquely utilize sub-100 nm wide lines as instructive surfaces for alignment and migration. Several studies have shown the ability of micro-channels to induce migratory directionality of cancer cells such as those of breast and prostate cancer.[24–26] However, to date little data have been reported on the influence of sub-100 nm lines on metastatic cancer cell. Our observations have implications for the development of lined nanotopographies at the sub-100 nm scale to further study metastatic cell behavior in a more physiologically relevant cell culture model. Interestingly, the collagen network of the bladder wall contains fibrils of diameters that are of similar dimension to the nanotopography investigated in our study. The inner mucosal layer of the bladder contains three distinct areas of collagen networks and underlies the epithelial cell layer which contains the precursor cells of most bladder cancers. Using SEM, Murakumo *et al.* showed that this mucosal layer is comprised of three different collagen networks that differ in arrangement, density, and size of collagen fibrils. The superficial layer is made up of a dense layer of thin collagen fibrils woven together to support the epithelial cell layer, with diameters ranging from 50 to 200 nm. The middle portion of the mucosal layer contains well-ordered parallel collagen bundles of 2–6 μm width, which are surrounded by individual collagen fibrils of 100–200 nm diameter. This layer is surrounded by twisted collagen bundles in the deep portion of the mucosal layer, which are able to stretch in response to bladder filling and are again surrounded by individual collagen fibrils in the 100 nm diameter range.[27]

Little information exists on the structural changes in these collagen fibril networks during metastatic progression, using SEM analysis. It has previously been shown that collagen networks are altered during breast cancer metastasis and that metastatic breast cancer cells use rearranged collagen fibrils in the ECM to migrate away from the primary tumor to nearby blood vessels.[6] During bladder metastatic progression it has been reported that infiltrating transitional bladder carcinomas significantly enhance the expression of ECM components, such as fibronectin and certain collagens, as well as matrix degrading proteases.[28,29] This suggests that metastatic bladder cancer cells may similarly influence the physical nature of the ECM, thereby facilitating their migration and invasion. In a scratch wound healing assay, we have shown that patterns mimicking the physical dimensions of collagen fibrils are able to

promote or inhibit migration based on the directionality of the underlying lined pattern in relation to the direction of the wound (Figure 3). 253J-BV cells use the lines as guides during migration when the wound is scratched orthogonal to the lines, whereas, when cells are forced to move perpendicular to the lines migration is greatly inhibited. This correlates with the previous report, which suggests that collagen fibrils act as guides for metastatic tumor cell migration.[6]

Many studies have examined the role of nano- and micro-printing of ECM components, such as fibronectin and collagen, as instructive surfaces for cellular attachment and migration.[5,30,31] Our data suggest that the physical dimensions of an underlying pattern at the sub-100 nm scale can induce anisotropy and migration of metastatic tumor cells without prior deposition of these matrix components. In a related study, it was shown that surface chemical cues (fibronectin) appear to affect initial settling down of osteoblast cells on 90 nm lines, while physical cues of the surface pattern have greater influence on cell adhesion and directionality.[20] 253J-BV have enhanced fibronectin production compared to 253J cells (Supplemental Figure 1), and it is likely that metastatic tumor cells are able to promote their deposition of this matrix protein to facilitate attachment to nanotopography via integrin engagement and focal contact turnover. It should be noted that although no ECM components were purposefully deposited on the nanotopography, seeding of cells occurred in supplemented media containing FBS, which contains ECM proteins. This likely provides further sites for integrin attachment on the topography.

Enhanced alignment and migration of metastatic 253J-BV cells was accompanied by increased appearance of filopodia along the cellular body and lamellipodial front when cultured on 65 nm lined topography (Figure 4). Filopodia are thin (100–300 nm diameter) membrane protrusions that are involved in probing the microenvironment during neuronal outgrowth, angiogenesis, wound healing, and migration.[32,33] Filopodia have also been implicated in sensing the physical environment of underlying topography for fibroblasts, endothelial cells, osteoblasts, and neurons.[34–42] Importantly, filopodia have been associated with migration through 3D matrices.[43–45] In addition to filopodia dynamics, the occurrence of focal contacts, as visualized by phospho-FAK (Y397), and actin stress fiber formation, was also altered in response to 253J-BV cells being cultured on 65 nm lined topography (Figure 5). Migration in 3D matrices is associated with smaller integrin clusters that rapidly dissociate and associate compared to large focal adhesions in cells migrating on a flat surface. Further, it has been shown that different proteins associated with the FAK signaling complex appear to have a differential regulatory roles depending whether the cell is undergoing migration over a 2D surface or a 3D environment.[2,3] While some components of the focal adhesion complex, such as FAK and p130cas, are involved in 3D migration speed and formation of membrane protrusions, others, such as zyxin, enhance migration only over 2D surfaces.[2] Interestingly, the FAK adaptor protein p130cas has also been associated with enhanced filopodia formation.[46–48] We have previously demonstrated that 253J-BV cells display enhanced phospho-p130cas-mediated migration, which is dependent on enhanced redox-mediated signaling within 253J-BV cells.[9] The role of p130cas in mediating filopodia formation in response to nanotopography warrants further investigation. These differences highlight the importance of considering the physical landscape of tumor cells in designing studies to examine molecular mechanisms that regulate tumor cell migration. Our work has shown that 3D patterns on the nanoscale can be used to mimic collagen fibrils in the ECM, providing a physically relevant instructive surface for the analysis of metastatic cancer cells.

Author Contributions: All authors participated in the design, interpretation of the studies, analysis of the data and review of the manuscript; JNI, PDK, and NJB conducted the experiments and JNI, PDK and NH wrote the manuscript.

ACKNOWLEDGEMENTS

We thank Drs Badar Mian (Albany Medical College) and Colin Dinney (M.D. Anderson Cancer Center) for generously providing 253J and 253J-BV cell lines. We are grateful to Drs J. Andres Melendez (CNSE) and Thomas Goodman for helpful discussions. We thank Drs Natalya Tokranova (CNSE) and Magnus Bergkvist (CNSE) for providing silicon wafers. Thanks to the following CNSE staff and students for helpful technical assistance: Alison Gracias, William Stephenson, Usawadee Dier, Dr Sabarinath Jayaseelan, and Michael Murphy. This work was supported by NIH grant R00CA143229 from the National Cancer Institute (to NH).

REFERENCES

1. Siegel R, Naishadham D, Jemal A. Cancer statistics, 2013. *CA Cancer J Clin* 2013;**63**:11–30
2. Fraley SI, Feng Y, Krishnamurthy R, Kim DH, Celedon A, Longmore GD, Wirtz D. A distinctive role for focal adhesion proteins in three-dimensional cell motility. *Nat Cell Biol* 2010;**12**:598–604
3. Friedl P, Zanker KS, Brocker EB. Cell migration strategies in 3-D extracellular matrix: differences in morphology, cell matrix interactions, and integrin function. *Microsc Res Tech* 1998;**43**:369–78
4. Martins GG, Kolega J. Endothelial cell protrusion and migration in three-dimensional collagen matrices. *Cell Motil Cytoskeleton* 2006;**63**:101–15
5. Kim DH, Provenzano PP, Smith CL, Levchenko A. Matrix nanotopography as a regulator of cell function. *J Cell Biol* 2012;**197**:351–60
6. Provenzano PP, Inman DR, Eliceiri KW, Trier SM, Keely PJ. Contact guidance mediated three- dimensional cell migration is regulated by Rho/ROCK-dependent matrix reorganization. *Biophys J* 2008;**95**:5374–84
7. Iyoki M, Araki K, Ogata T. Scanning electron microscopic study of the three-dimensional structure of the collagen networks of gastric cancer. *Scanning Microsc* 1994;**8**:365–73
8. Zunich SM, Valdovinos M, Douglas T, Walterhouse D, Iannaccone P, Lamm ML. Osteoblast-secreted collagen upregulates paracrine Sonic hedgehog signaling by prostate cancer cells and enhances osteoblast differentiation. *Mol Cancer* 2012;**11**:30
9. Hempel N, Bartling TR, Mian B, Melendez JA. Acquisition of the metastatic phenotype is accompanied by H2O2-dependent activation of the p130Cas signaling complex. *Mol Cancer Res* 2013;**11**:303–12
10. Hempel N, Ye H, Abessi B, Mian B, Melendez JA. Altered redox status accompanies progression to metastatic human bladder cancer. *Free Radic Biol Med* 2009;**46**:42–50

11. Dinney CP, Fishbeck R, Singh RK, Eve B, Pathak S, Brown N, Xie B, Fan D, Bucana CD, Fidler IJ, Killion JJ. Isolation and characterization of metastatic variants from human transitional cell carcinoma passaged by orthotopic implantation in athymic nude mice. *J Urol* 1995;**154**:1532–8
12. Gupton SL, Gertler FB. Filopodia: the fingers that do the walking. *Sci STKE* 2007;**2007**:re5
13. Jiang F, Horber H, Howard J, Muller DJ. Assembly of collagen into microribbons: effects of pH and electrolytes. *J Struct Biol* 2004;**148**:268–78
14. Prockop DJ, Kivirikko KI. Collagens: molecular biology, diseases, and potentials for therapy. *Annu Rev Biochem* 1995;**64**:403–34
15. Loesberg WA, te Riet J, van Delft FC, Schon P, Figdor CG, Speller S, van Loon JJ, Walboomers XF, Jansen JA. The threshold at which substrate nanogroove dimensions may influence fibroblast alignment and adhesion. *Biomaterials* 2007;**28**:3944–51
16. Diehl KA, Foley JD, Nealey PF, Murphy CJ. Nanoscale topography modulates corneal epithelial cell migration. *J Biomed Mater Res A* 2005;**75**:603–11
17. Teixeira AI, McKie GA, Foley JD, Bertics PJ, Nealey PF, Murphy CJ. The effect of environmental factors on the response of human corneal epithelial cells to nanoscale substrate topography. *Biomaterials* 2006;**27**:3945–54
18. Teixeira AI, Abrams GA, Bertics PJ, Murphy CJ, Nealey PF. Epithelial contact guidance on well-defined micro- and nanostructured substrates. *J Cell Sci* 2003;**116**:1881–92
19. Fujita S, Ohshima M, Iwata H. Time-lapse observation of cell alignment on nanogrooved patterns. *J R Soc Interface* 2009;**6**:S269–77
20. Tsai WB, Ting YC, Yang JY, Lai JY, Liu HL. Fibronectin modulates the morphology of osteoblast-like cells (MG-63) on nano-grooved substrates. *J Mater Sci Mater Med* 2009;**20**:1367–78
21. Yang JY, Ting YC, Lai JY, Liu HL, Fang HW, Tsai WB. Quantitative analysis of osteoblast- like cells (MG63) morphology on nanogrooved substrata with various groove and ridge dimensions. *J Biomed Mater Res A* 2009;**90**:629–40
22. Palama IE, D'Amone S, Coluccia AM, Gigli G. Micropatterned polyelectrolyte nanofilms promote alignment and myogenic differentiation of C2C12 cells in standard growth media. *Biotechnol Bioeng* 2013;**110**:586–96
23. Ranjan A, Webster TJ. Increased endothelial cell adhesion and elongation on micron-patterned nano-rough poly(dimethylsiloxane) films. *Nanotechnology* 2009;**20**:305102
24. Mak M, Reinhart-King CA, Erickson D. Microfabricated physical spatial gradients for investigating cell migration and invasion dynamics. *PLoS One* 2011;**6**:e20825
25. Rolli CG, Seufferlein T, Kemkemer R, Spatz JP. Impact of tumor cell cytoskeleton organization on invasiveness and migration: a microchannel-based approach. *PLoS One* 2010;**5**:e8726
26. Sarna M, Wybieralska E, Miekus K, Drukala J, Madeja Z. Topographical control of prostate cancer cell migration. *Mol Med Rep* 2009;**2**:865–71
27. Murakumo M, Ushiki T, Abe K, Matsumura K, Shinno Y, Koyanagi T. Three-dimensional arrangement of collagen and elastin fibers in the human urinary bladder: a scanning electron microscopic study. *J Urol* 1995;**154**:251–6
28. Wetzels RH, Robben HC, Leigh IM, Schaafsma HE, Vooijs GP, Ramaekers FC. Distribution patterns of type VII collagen in normal and malignant human tissues. *Am J Pathol* 1991;**139**:451–9
29. Aitken KJ, Bagli DJ. The bladder extracellular matrix. *Part I: architecture, development and disease.* Nat Rev Urol 2009;**6**:596–611
30. Doyle AD, Wang FW, Matsumoto K, Yamada KM. One-dimensional topography underlies three-dimensional fibrillar cell migration. *J Cell Biol* 2009;**184**:481–90
31. Pouthas F, Girard P, Lecaudey V, Ly TB, Gilmour D, Boulin C, Pepperkok R, Reynaud EG. In migrating cells, the Golgi complex and the position of the centrosome depend on geometrical constraints of the substratum. *J Cell Sci* 2008;**121**:2406–14
32. Ridley AJ. Life at the leading edge. *Cell* 2011;**145**:1012–22
33. Mattila PK, Lappalainen P. Filopodia: molecular architecture and cellular functions. *Nat Rev Mol Cell Biol* 2008;**9**:446–54
34. Clark P, Connolly P, Curtis AS, Dow JA, Wilkinson CD. Topographical control of cell behaviour: II. *Multiple grooved substrata.* Development 1990;**108**:635–44
35. Dalby MJ, Gadegaard N, Riehle MO, Wilkinson CD, Curtis AS. Investigating filopodia sensing using arrays of defined nano-pits down to 35 nm diameter in size. *Int J Biochem Cell Biol* 2004;**36**:2005–15
36. Dalby MJ, Marshall GE, Johnstone HJ, Affrossman S, Riehle MO. Interactions of human blood and tissue cell types with 95-nm-high nanotopography. *IEEE Trans Nanobiosci* 2002;**1**:18–23
37. Dalby MJ, Pasqui D, Affrossman S. Cell response to nano-islands produced by polymer demixing: a brief review. *IEE Proc Nanobiotechnol* 2004;**151**:53–61
38. Dalby MJ, Riehle MO, Johnstone H, Affrossman S, Curtis AS. Investigating the limits of filopodial sensing: a brief report using SEM to image the interaction between 10 nm high nano- topography and fibroblast filopodia. *Cell Biol Int* 2004;**28**:229–36
39. Dalby MJ, Riehle MO, Sutherland DS, Agheli H, Curtis AS. Changes in fibroblast morphology in response to nano-columns produced by colloidal lithography. *Biomaterials* 2004;**25**:5415–22
40. Dalby MJ, Yarwood SJ, Johnstone HJ, Affrossman S, Riehle MO. Fibroblast signaling events in response to nanotopography: a gene array study. *IEEE Trans Nanobiosci* 2002;**1**:12–7
41. Rajnicek A, Britland S, McCaig C. Contact guidance of CNS neurites on grooved quartz: influence of groove dimensions, neuronal age and cell type. *J Cell Sci* 1997;**110**:2905–13
42. Rajnicek A, McCaig C. Guidance of CNS growth cones by substratum grooves and ridges: effects of inhibitors of the cytoskeleton, calcium channels and signal transduction pathways. *J Cell Sci* 1997;**110**:2915–24
43. Soll DR, Voss E, Johnson O, Wessels D. Three-dimensional reconstruction and motion analysis of living, crawling cells. *Scanning* 2000;**22**:249–57
44. Heath JP, Peachey LD. Morphology of fibroblasts in collagen gels: a study using 400 keV electron microscopy and computer graphics. *Cell Motil Cytoskeleton* 1989;**14**:382–92
45. Pang Y, Wang X, Lee D, Greisler HP. Dynamic quantitative visualization of single cell alignment and migration and matrix remodeling in 3-D collagen hydrogels under mechanical force. *Biomaterials* 2011;**32**:3776–83
46. Cho SY, Klemke RL. Purification of pseudopodia from polarized cells reveals redistribution and activation of Rac through assembly of a CAS/Crk scaffold. *J Cell Biol* 2002;**156**:725–36
47. Gustavsson A, Yuan M, Fallman M. Temporal dissection of beta1-integrin signaling indicates a role for p130Cas-Crk in filopodia formation. *J Biol Chem* 2004;**279**:22893–901
48. Kiyokawa E, Matsuda M. Regulation of focal adhesion and cell migration by ANKRD28DOCK180 interaction. *Cell Adhes Migration* 2009;**3**:281–4

(Received July 2, 2014, Accepted October 8, 2014)